CHEMISTRY OF MATERIALS

ARTICLE

pubs.acs.org/cm

Aerosol-Assisted Chemical Vapor Deposition of Transparent Conductive Gallium−Indium−Oxide Films

Caroline E. Knapp, Geoffrey Hyett, Ivan P. Parkin, and Claire J. Carmalt*

Materials Chemistry Centre, Department of Chemistry, University College London, 20 Gordon Street, London WC1H 0AJ, U.K.

Supporting Information

ABSTRACT: Aerosol assisted chemical vapor deposition (AACVD) reactions of $GaMe_3$, $InMe_3$, and 6 equiv of the donor functionalized alcohol, $HOCH_2CH_2OMe$, in toluene resulted in the deposition of colorless, transparent gallium−indium−oxide films at a range of temperatures (350−450 °C). The gallium−indium−oxide films were analyzed by a range of techniques including scanning electron microscopy (SEM), atomic force microscopy (AFM), X-ray photoelectron spectroscopy (XPS), glancing-angle X-ray powder diffraction (XRD), and wavelength dispersive analysis of X-rays (WDX). The optimum growth temperature was found to be 450 °C, which produced transparent films with a composition of $Ga_{0.6}In_{1.4}O_3$ as determined by WDX. XPS confirmed the presence of indium, gallium, and oxygen in the films. Annealing these films at 1000 °C resulted in crystalline films, and glancing-angle powder XRD showed a gallium-substituted cubic In_2O_3 lattice was adopted with a lattice parameter, a = 9.84 Å. AFM showed that the annealed films on quartz had a root-mean-square roughness of 94−200 nm, and the work function was measured to be 4.6 eV. The four point probe method was used to determine a sheet resistivity, R_s = 83.3 Ω/square, and a low electrical resistivity value (for example 6.66×10^{-4} Ω cm in 80 nm sample thickness, as determined by side-on SEM for films deposited on glass).

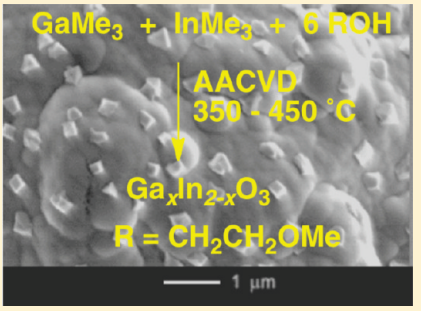

KEYWORDS: gallium indium oxide, transparent conducting oxide, thin film, AACVD

INTRODUCTION

Interest in transparent conducting oxides (TCOs) over the past two decades has increased dramatically due to their application in optoelectronic devices such as photovoltaics, solar cells, flat panel displays, and OLED screens.[1] TCO properties can be assigned to the basic relationships between their transparency, structure, and composition and the atomic arrangements of the metal cations in both crystalline and amorphous oxide structures.[2,3] TCOs display the remarkable combination of optical transparency and high electrical conductivity. A number of reviews on TCOs,[3] including processing approaches, the design of these materials, and new techniques for improving transmissivity in the films have been published.[4]

The material typically used as the anode in the OLED screen and other such technologies is a thin layer of indium tin oxide (ITO) or fluorinated tin oxide,[5,6] although a large number of other TCO materials are known, for example tin oxide. However, their properties, including low resistivity, good transparency, availability, and also the ease with which it can be patterned are dwarfed in comparison to the performance of ITO. The aforementioned TCOs, most notably ITO, are largely used in photovoltaic technologies as well as being components of display technologies. Recently, multicomponent ternary and quaternary oxide wide band gap semiconductors have been investigated as new materials for transparent conducting films and as materials for thin film transistor (TFT) channel layers.

In an attempt to improve TCO film electrical, optical, and chemical properties a number of studies have focused on doping various metal oxide combinations of In, Sn, Zn, Al, and Ga.[7,8] Indeed, gallium−indium−oxide is the reported parent phase of a promising, relatively unexplored TCO family.[9] An advantage that gallium−indium−oxide has over ITO is its improved transmission in the blue-green region of the electromagnetic spectrum.[10] There are few reports in the literature of the synthesis of phase pure gallium−indium−oxide,[11] and even less for the production of thin films of these materials.[12] Solid solutions based on XRD data of $In_{2x}Ga_{2-2x}O_3$ where $x \leq 0.43$ results in indium substitution into the β-Ga_2O_3 lattice and $x \geq 0.95$ results in gallium substitution into the cubic In_2O_3 lattice. Any other In:Ga ratios have resulted in the presence of mixed phases.[13] In an earlier study thin films of $In_xGa_{2-x}O_3$ prepared by dc magnetron sputtering were found to be amorphous, only adopting the β-Ga_2O_3 crystal structure.[13] The charge transport and transparency of gallium−indium−oxide grown by heteroepitaxial metalorganic chemical vapor deposition with O_2 as the oxidizing gas have also been reported.[9] It was shown here that the optical transmission window of these films was considerably broader than that of ITO, and the absolute transparency rivals or exceeds that of the most transparent conductive oxides known.

Received: August 11, 2010
Revised: January 28, 2011
Published: March 02, 2011

ACS Publications © 2011 American Chemical Society

The applications of TCO materials largely require the material as thin films, and chemical vapor deposition (CVD) is one of the most practical methods for preparing thin films for large-scale applications.[14] CVD has a number of advantages over other deposition techniques as it offers the potential for good film uniformity and composition control, large area growth, and excellent step coverage. This paper describes the first aerosol-assisted (AA) CVD of gallium−indium−oxide thin films.[15] Due to the influence of the solvent on the deposition, AACVD can lead to unique or different morphologies that could potentially result in improved properties.[16,17] In addition, only minimal amounts of precursor (ca. 0.5 g) are required, and thin films can be deposited under AACVD conditions at low temperatures.[18] AACVD uses a liquid−gas aerosol to transport soluble precursors to a heated substrate and is a useful method when a conventional atmospheric pressure CVD precursor proves involatile or thermally unstable.[19]

Herein, we report the formation of $Ga_xIn_{2-x}O_3$ thin films by AACVD from the in situ reaction of $GaMe_3$, $InMe_3$, and the donor-functionalized alcohol $HOCH_2CH_2OMe$ in toluene. No oxygen carrier gas was necessary, and the films could be crystallized *via* a simple annealing step. We show that it is possible to grow thin $Ga_xIn_{2-x}O_3$ films that are transparent and conductive.

EXPERIMENTAL SECTION

Caution. It should be noted that $GaMe_3$ and $InMe_3$ are pyrophoric substances, which ignite spontaneously in air, and the CVD of these chemicals can potentially be toxic and corrosive. All experiments should be conducted in a fume hood. Following the deposition, films are air and moisture stable and are safe to handle as any reactive species leave via the reactor exhaust during the AACVD process.

General Procedures. Depositions were carried out under dinitrogen (99.99% from BOC). Precursors were placed in an AACVD glass bubbler, and an aerosol mist was created using a piezo electric device. The solvent mist was transported in a flow of cold nitrogen from the bubbler in an 8-mm gauge pipe to a horizontal bed, cold-wall reactor (internal dimensions 15 cm × 5 cm) fitted with a graphite block containing a Whatman cartridge heater, used to heat the glass substrate. The temperature of the substrate was monitored by a Pt−Rh thermocouple. Depositions were carried out by heating the horizontal bed reactor to the required temperature before diverting the nitrogen line through the aerosol and hence to the reactor. The glass substrate was SiO_2, precoated (ca. 50 nm thick SiO_2 barrier layer) standard float glass (Pilkington, U.K.) 15 cm ×4 cm × 0.3 cm. A sheet of polished quartz (4 cm ×1.5 cm × 0.1 cm) was placed on the substrate 2 cm from the front of the reactor to enable a subsequent annealing step at 1000 °C. A top plate was suspended 0.5 cm above the glass substrate to ensure a laminar flow. Temperature gradient measurements have shown there to be a temperature difference of 50−70 °C between the top and the bottom plates.

The substrates were cleaned prior to use, to remove surface grease. Two-way taps were used to divert the nitrogen carrier gas through the bubbler, and the aerosol was carried into the reactor in a stream of nitrogen gas through a brass baffle to obtain a laminar flow. The total time for the deposition process was in the region of 30−90 min. At the end of the deposition the nitrogen flow through the aerosol was diverted, and only nitrogen passed over the substrate. The glass substrate was allowed to cool with the graphite block to less than 100 °C before it was removed. Coated substrates were handled and stored in air. Large pieces of glass (ca. 4 cm × 2 cm) were used for X-ray powder diffraction. The coated glass substrate was cut into ca. 1 cm ×1 cm squares for subsequent analysis by scanning electron microscopy (SEM), wavelength dispersive analysis of X-rays (WDX), and energy dispersive analysis of X-rays (EDX).

Scheme 1. AACVD Reaction of $GaMe_3$, $InMe_3$, and $HOCH_2CH_2OMe$

$$GaMe_3 + InMe_3 + 6\ HOCH_2CH_2OMe \xrightarrow[350-450°C]{\text{AACVD}} Ga_xIn_{2-x}O_3$$

$$x = 0.6 - 1.2$$

Film Analysis Methods. Powder XRD patterns were measured on a Siemens D5000 diffractometer using monochromated Cu $K\alpha_1$ radiation ($K\alpha_1$ = 1.5406 Å). The diffractometer used glancing incident radiation (1.5°). The samples were indexed using the GSAS program, refined via the Rietveld method, and compared to database standards. EDAX was obtained on a Philips XL30ESEM instrument and SEM on a JEOL 6301 instrument. UV−vis−NIR spectra were recorded in the range 190−1100 nm using a Helios double beam instrument. Reflectance and transmission spectra were recorded between 300 and 2300 nm by a Zeiss miniature spectrometer. Reflectance measurements were standardized relative to a rhodium mirror and transmission relative to air. Atomic force microscopy (AFM) was used to measure the surface topology and root mean squared (rms) roughness of the selected gallium−indium−oxide films. All films were scanned for 16 and 20 μm field sizes. The mean rms roughness values were obtained. A Kelvin probe measurement estimated the work function of films to be 4.6 eV, which is comparable to ITO and films of gallium−indium−oxide deposited via other techniques.[2,9]

AACVD Reaction of $GaMe_3$, $InMe_3$, and $HOCH_2CH_2OMe$. The precursor solution was generated in situ from the reaction of $GaMe_3$, $InMe_3$, and excess $HOCH_2CH_2OMe$ in toluene. Trimethylgallium and trimethylindium were supplied by SAFC Hitech and used without further purification. $HOCH_2CH_2OMe$ was procured from Aldrich and was distilled, degassed, and stored over molecular sieves. Excess alcohol was used to minimize the risk of producing partially oxidized films. $GaMe_3$ (1.0094 g, 8.8 mmol) and $InMe_3$ (1.3897 g, 8.7 mmol) were cooled to −78 °C and each dissolved in precooled toluene (ca. 15 cm^3) at −78 °C. These were added dropwise to an AACVD flask along with the dropwise addition of $HOCH_2CH_2OMe$ (6.2 cm^3, 0.052 mol). The reaction mixture was allowed to sit for ca. 10 min before the deposition was started. Depositions were carried out at a flow rate of 1.0 L min^{-1} over a range of substrate temperatures (350−450 °C). Deposition times for each experiment ranged 60−120 min. After deposition the bubbler was closed and the substrate allowed to cool under flow of nitrogen. Quartz sheets were annealed for 1 and 12 h at 1000 °C. The flow rate was experimented with and optimized at 1 L/min; a variety of solvents were also tested (e.g., hexanes, dichloromethane), but toluene proved the most successful at producing uniform films with good substrate coverage. A variety of substrates (glass, opaque, and polished quartz) were used so that annealing effects could be observed. The same procedure was used for the AACVD reaction of $GaMe_3$, $InMe_3$, and $HOCH_2CH_2OMe$ at deposition temperatures ranging from 350 to 450 °C.

RESULTS AND DISCUSSION

Transparent films of gallium indium oxide have been deposited on glass from the AACVD reaction of $GaMe_3$, $InMe_3$, and the donor-functionalized alcohol $HOCH_2CH_2OMe$, according to Scheme 1. The reaction of $GaMe_3$, $InMe_3$, and $HOCH_2CH_2OMe$ in toluene presumably generated in situ dimethylalkoxometallanes,

Table 1. Deposition Conditions and Analysis of the Films Grown from the AACVD of $GaMe_3$, $InMe_3$, and ROH (R = CH_2CH_2OMe) in Toluene

precursors	T [°C]	T annealed [°C]	WDX	thickness [nm]	resistivity [Ω cm]
$GaMe_3$, $InMe_3$, ROH	350		$Ga_{1.2}In_{0.8}O_{2.4}$		too thin
$GaMe_3$, $InMe_3$, ROH	350	550	$Ga_{1.0}In_{1.0}O_{2.9}$		too thin
$GaMe_3$, $InMe_3$, ROH	400	550			too thin
$GaMe_3$, $InMe_3$, ROH	450		$Ga_{0.6}In_{1.4}O_{3.4}$	80	6.6×10^{-4}
				90	7.5×10^{-4}
$GaMe_3$, $InMe_3$, ROH	450	1000[a]	$Ga_{0.6}In_{1.4}O_{3.1}$	100	8.8×10^{-4}
				110	9.2×10^{-4}
				120	10.0×10^{-4}

[a] Quartz substrates.

of the type $[Me_2M(OR)]_n$ (M = Ga, In), based on related solution phase reactions we have described previously.[16,17,20] The AACVD reaction of $GaMe_3$, $InMe_3$, and $HOCH_2CH_2OMe$ on glass and quartz substrates was studied at 350−450 °C. For each system, deposition was observed on both the substrate and the top plate, which is the glass plate that rests 8 mm above the surface of the substrate. Films deposited on the substrate were used in the analysis below. Deposition on the substrate and top plate is a result of the thermophoretic force that gas-phase particles are subjected to during AACVD. Since the flow of gas in the reactor is laminar rather than turbulent, thermophoresis is usually the dominant force in determining the deposition location of particles; hence, deposition also occurs on the elevated surfaces above the actual surface that requires coating. The top plate was measured to be ∼50−70 °C lower in temperature than the bottom plate.

The films deposited at all temperatures were uniform, and there was good coverage of the substrate, with those deposited at 450 °C showing the best coverage of the substrate, with a complete conformal coating. The films were adherent to the substrate, passing the Scotch Tape test. However, they were readily scratched by a brass or stainless steel stylus. The as-deposited films were amorphous as shown by glancing-angle powder X-ray diffraction (XRD). The as-deposited films had a brown tint, which suggests some carbon contamination in the films. Annealing the films at temperatures as low as 550 °C removed the brown color and yielded transparent films, although the films were still X-ray amorphous. A higher temperature anneal at 1000 °C (films deposited on quartz substrates) was necessary to crystallize the films (vide infra). Solubility testing of the films was carried out in organic solvents (ethanol, methanol, toluene, THF, and DCM) and also under acidic conditions (16 M HNO_3). The films suspended in the organic solvents showed no change while those in nitric acid were completely removed after 24 h. The deposition conditions and analysis of the films grown are given in Table 1.

The gallium−indium−oxide films were characterized using a range of techniques. Glancing-angle X-ray diffraction (XRD) showed that the films deposited by AAVCD were amorphous at all deposition temperatures. The deposition of amorphous films at these temperatures is typical for gallium oxide, where crystalline films are only afforded at higher deposition temperatures (>650 °C).[21−24] With particular relevance to this study, we have previously described the AACVD of $GaMe_3$ and $HOCH_2CH_2OMe$ at 450 °C, which resulted in the formation of amorphous thin films of Ga_2O_3 on glass substrates.[24] In contrast, the AACVD reaction of $InMe_3$ and $HOCH_2CH_2OMe$ under similar conditions yielded cubic crystalline In_2O_3 films.[16] Thus, the presence of gallium in these films has resulted in the formation of amorphous films. The as-deposited films were annealed at 550 °C; however, they remained amorphous. The films deposited at 450 °C showed the best coverage and so were also deposited on quartz substrates. These films were annealed at 1000 °C, which resulted in highly transparent films, and glancing-angle XRD showed that they were not monoclinic but consisted of a Ga-substituted cubic In_2O_3 microstructure, as shown in Figure 1.

X-ray diffraction data were collected from the film in the range of $10° < 2\theta < 60°$, which produced a pattern with three broad Bragg peaks at 31.2°, 36.5°, and 52.4° 2θ, as well as a broad feature centered at 21.9° 2θ due to scattering from the amorphous glass substrate. The three Bragg peaks could be indexed using the cubic space group $Ia3$ with a lattice parameter of a = 9.85 Å. Under ambient conditions In_2O_3 also indexes in this space group, but with a lattice parameter of 10.12 Å,[25] while Ga_2O_3 is found in $R3ch$ with a lattice parameters of a = 4.98 Å and c = 13.43 Å.[26] As the film is found to crystallize in the same space group as In_2O_3 but with a reduced lattice parameter of 9.85 Å this strongly indicates that the film is comprised of a mixed gallium−indium−oxide, with the indium oxide structure, but partial substitution of indium ions (r = 0.8 Å) with the smaller gallium ion (r = 0.62 Å) causing a reduction in the unit cell.[27] A Rietveld refinement using the diffraction pattern was conducted with the In_2O_3 structure as a starting model but modified with a smaller unit cell and the two crystallographic metal sites (8b and 24d) containing both indium and gallium ions, as determined from EDX measurements. This produced an acceptable fit to the data (χ^2 of 35.6). However, this model of the In_2O_3 structure predicted three peaks between 37 and 48° 2θ which were not observed in the data. It was found that a modification of the structure by shifting the 24d metal ion eliminated these peaks and produced a significantly better fit (χ^2 of 19.5). In_2O_3 crystallizes in the C type rare earth sesquioxide structure, which itself is based upon the fluorite structure, with a doubled unit cell to accommodate the reduced ratio of anions and a periodic distortion in the indium ion positions. The introduction of gallium into the structure of the thin film seems to eliminate this periodic distortion in the metal lattice (modeled by the shift in the position of the metal ion). This is probably due to a disordered distribution of the indium and gallium across the metal sites.

The XRD patterns showed strong reflections from the (222) plane and preferred orientation along this plane is common for indium oxide.[16] The lattice parameter obtained can also be compared with that obtained for In_2O_3 films produced from

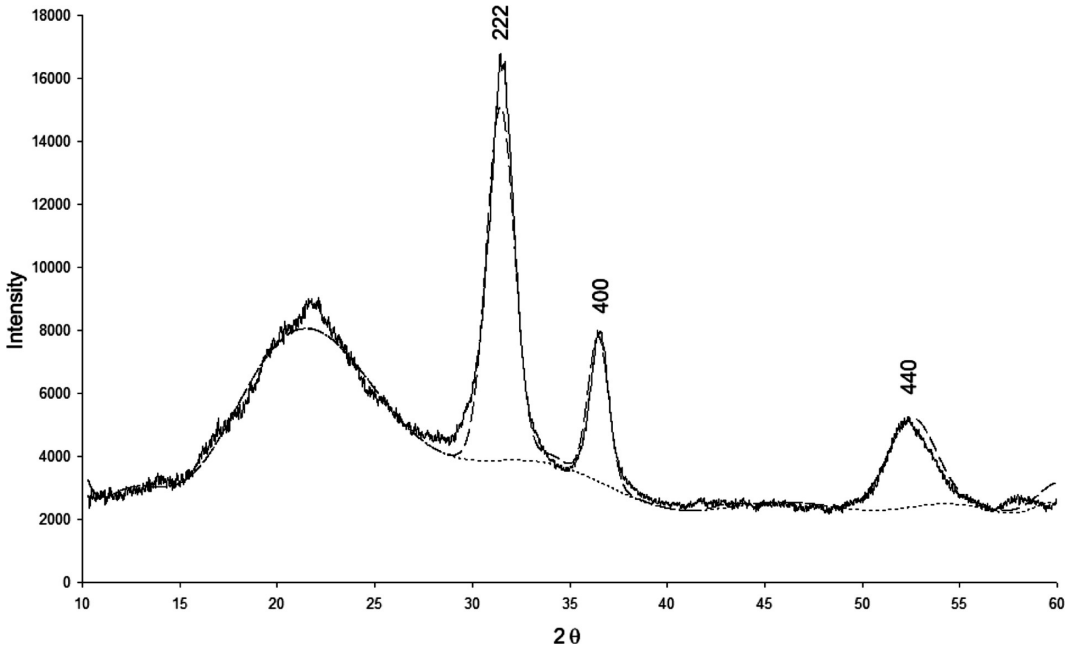

Figure 1. XRD pattern for film deposited on quartz at 450 °C and annealed at 1000 °C. Solid line indicates experimental data, dashed line indicates refinement and dotted line indicates background fit.

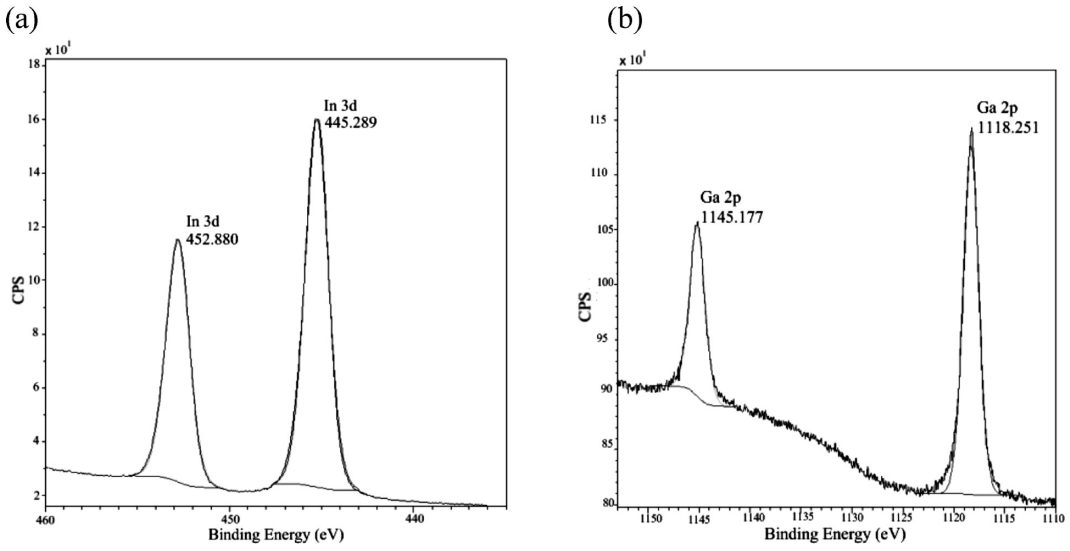

Figure 2. XPS of (a) In 3d peaks and (b) Ga 2p peaks for a film deposited at 450 °C by the in situ AACVD reaction of $GaMe_3$, $InMe_3$, and excess $HOCH_2CH_2OMe$ in toluene.

the AACVD reaction of $InMe_3$ and $HOCH_2CH_2OMe$, where a = 10.118 Å.[16] No peaks were observed for gallium oxide in the XRD pattern, which provides evidence that the gallium present (vide infra) is substituted in the indium oxide lattice. The X-ray powder diffraction patterns varied little between films, but in all instances peaks were observed to be wide, which can be a consequence of low angle XRD. However, XRD previously reported for Ga-substituted In_2O_3 also showed that XRD reflections are weaker and broader as the Ga content increases in the films (Ga/(Ga + In) > 12%). This is consistent with these films where the Ga content was (Ga/(Ga + In)) 30%. It is possible that the wide peaks observed are in fact multiple peaks indicative of mixtures of similar phases of the material; however, the analysis described below does not give evidence to support this, suggesting that only one phase is present (gallium-doped indium oxide). There is no evidence of phase separation, consistent with previous reports for $Ga_xIn_{2-x}O_3$ where phase separation (monoclinic β-Gallia) was only observed when Ga is substituted beyond $x \sim 1.1$ (in these films $x \sim 0.6$).

X-ray photoelectron spectroscopy (XPS) was used to analyze the surface of the films deposited at 450 °C and annealed at 1000 °C. XPS of the films revealed In 3d peaks at 445.3 and 452.9 eV corresponding to the In $3d_{5/2}$ and $3d_{3/2}$ peaks of In_2O_3, respectively (Figure 2a). These values are in close agreement with literature values previously reported for In_2O_3.[16,28] XPS also showed shifts at 1145.2 and 1118.3 eV, corresponding to Ga $2p_{1/2}$ and $2p_{3/2}$, respectively (Figure 2b). These values are consistent with literature reports for Ga_2O_3 peaks, and the XPS results

dx.doi.org/10.1021/cm102292b |*Chem. Mater.* 2011, 23, 1719–1726

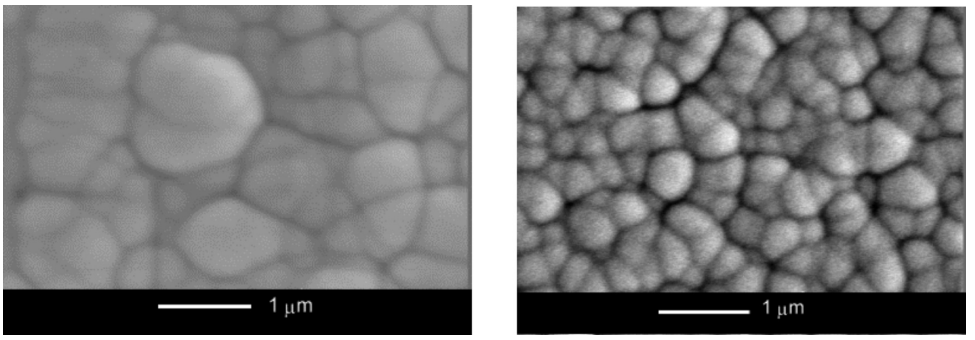

Figure 3. SEM images of gallium indium oxide films deposited on glass at (a) 350 °C and (b) 450 °C.

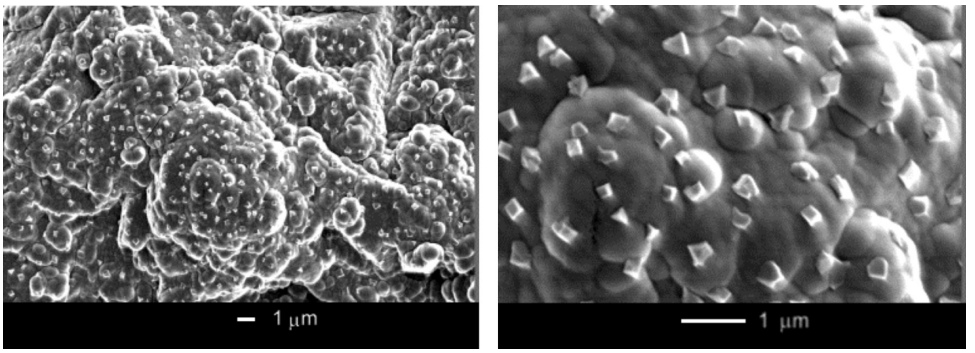

Figure 4. SEM images of gallium indium oxide film deposited on quartz at 450 °C and annealed for 12 h at 1000 °C.

therefore provide further evidence for the incorporation of gallium in the indium lattice of the films.[29]

XPS also showed that the O 1s peak of the same film could be deconvoluted into two components, which is similar to previous reports for In_2O_3.[27] The observed O 1s peak at 530.8 eV can be assigned to the lattice oxygen in crystalline In_2O_3, and the O 1s peak at 532.7 eV corresponds to adsorbed OH groups on the surface. A small peak was also observed corresponding to the C 1s environment, suggesting the presence of carbon at the surface of the film. However, it is likely that carbon contamination is low (<5 atom%) as described below.

Energy dispersive X-ray analysis (EDXA) confirmed the presence of gallium, indium, and oxygen in the films produced. However, breakthrough to the underlying glass substrate was observed, so metal to oxygen ratios could not be deduced accurately. No carbon was detected, so carbon contamination levels as a direct result of the precursors used are low (<5 atom%).

The composition of the films was further determined by wavelength dispersive X-ray (WDX) analysis. WDX analysis showed that the as-deposited films had an overall M:O ratio close to the expected 1:1.5 for M_2O_3. Deviations from the M_2O_3 stoichiometry occurred (1:1.7) with the formation of thinner films, which resulted in breakthrough to the underlying glass inhibiting accurate compositional analysis. Unfortunately, films grown at 400 °C (annealed at 550 °C) were too thin to analyze by WDX, and so no compositional formula was obtained; however, EDXA showed they contained gallium, indium, and oxygen (vide supra). Annealing the films at 550 °C did not crystallize the films or significantly change the composition. However, annealing the films at 1000 °C did result in crystalline films, although WDX showed that the as-deposited (450 °C) and annealed films (1000 °C) have a similar composition ($Ga_{0.6}In_{1.4}O_3$, Table 1). Annealing at 1000 °C in air seems to stabilize the framework as well as crystallize the films.

Scanning electron microscopy (SEM) was used to examine the surface morphology of the films and measure the film thickness. All the films as-deposited were composed of uniform clusters agglomerated together, regardless of the temperature of deposition. SEM of the films indicated that deposition occurred via an island growth mechanism (Figure 3). Annealing the films to 1000 °C for 12 h resulted in the formation of crystallite regions of size ca. 200 nm in diameter (Figure 4). The amorphous regions of the film are comparable to preannealed films. Area and spot analysis by WDX showed that the amorphous and crystallite regions of the annealed films had the same film composition. Interestingly, films that were annealed for longer periods of time (e.g., 24 h) exhibited the same morphology with amorphous and crystallite regions. However, films that were annealed for 1 h at 1000 °C showed a morphology somewhere between amorphous and crystalline, exhibiting sharpened edges with no distinct crystallite regions (Figure 5). Annealing the films deposited at 550 °C did not change the morphology.

Film thickness measurements by SEM for films deposited on glass at 450 °C gave a depth range of 80 nm up to 120 nm, with the thicker areas found at the center of the substrate.

Atomic force microscopy (AFM) was used to complement SEM and gain information about the film roughness. Figure 6 shows AFM images of gallium−indium−oxide films deposited on quartz at 450 °C and annealed at 1000 °C. AFM analysis of the gallium−indium−oxide films yielded low root mean squared (rms) roughness values, all averaging orders of magnitude lower than 1 μm. No trend in surface roughness was seen upon consecutive decreases in the field size of the analysis. Films were found to have a variety of rms roughness values, and while some samples had low rms roughness (94 nm) many others exhibited

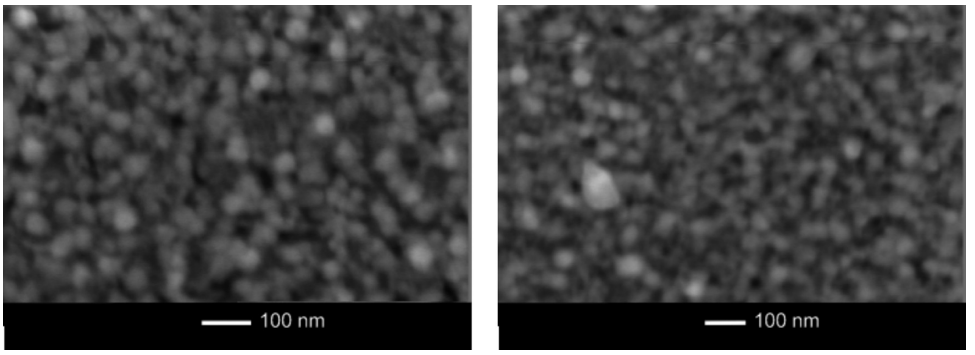

Figure 5. SEM images of gallium indium oxide film deposited on quartz at 450 °C and annealed for 1 h at 1000 °C.

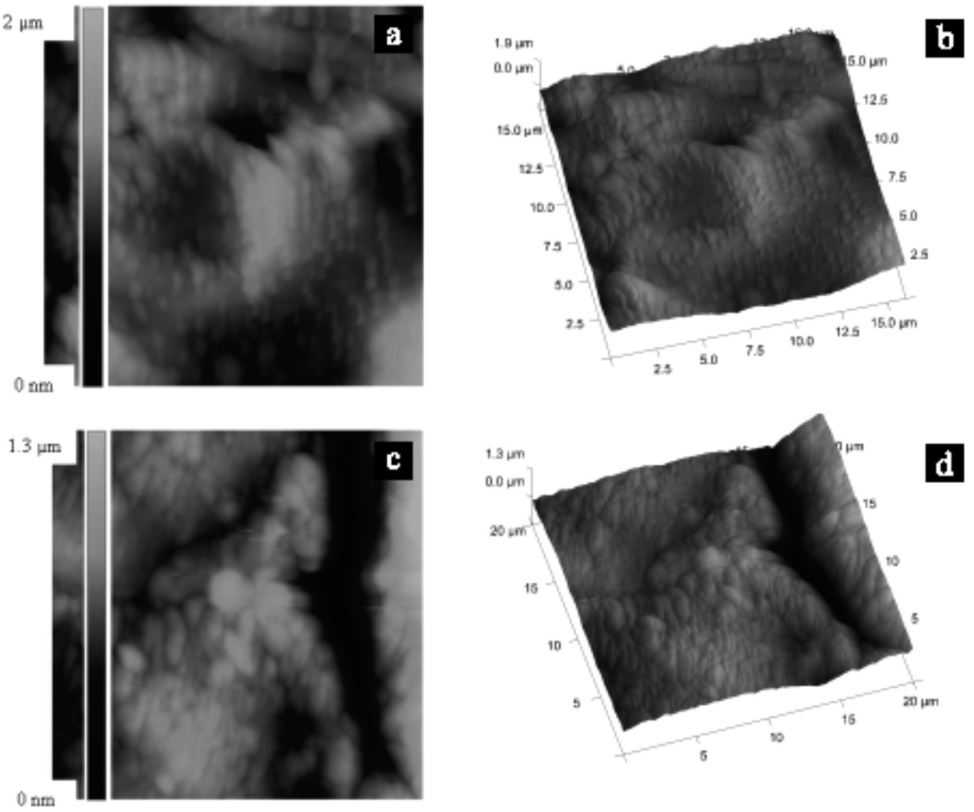

Figure 6. (a) 16 μm field size AFM image rms roughness =203 nm. (b) 3D image of the same area. (c) 20 μm field size AFM image rms roughness = 224 nm. (d) 3D image of the same area. All films deposited at 450 °C and annealed at 1000 °C.

roughness, which exceeded 200 nm (Figure 6). Typical rms roughness values in industrial application are below 100 nm.[6] The films analyzed by AFM were the annealed films deposited on quartz at 450 °C and annealed at 1000 °C, used for the XRD analysis. This is in contrast to those used for the film thickness measurements by side-on SEM, which were deposited on glass (also at 450 °C) and afforded smoother films.

A Kelvin probe measurement was used to estimate the work function of the gallium−indium−oxide thin films. The work function was measured to be 4.6 eV. This is consistent with reports of gallium−indium−oxide in the literature (4−5 eV)[9] and is comparable with ITO (4.5−5 eV).[6]

The optical properties of the films were studied by transmission and reflectance measurements between 300 and 2300 nm and by UV/visible spectroscopy between 90 and 1100 nm. All films showed a slight shift in the adsorption edge toward the visible relative to a plain glass substrate. The gallium−indium−oxide films displayed minimal reflectivity (5−10%) and high transmission (80−90%). The reflectance was high in the mid-UV and visible regions (80−90%). Conducting a Tauc plot[30] of the UV/visible data indicated that the bandgap of the films varied from 3.7 to 4.6 eV, as the amount of gallium doping increased. Therefore, the films deposited at 450 °C with a composition of $Ga_{0.6}In_{1.4}O_{3.1}$, which adopt the cubic-In_2O_3 framework, showed band gaps of ∼3.7 eV comparable to literature values for In_2O_3.[9] The larger band gaps suggest the formation of a Ga_2O_3 framework, as the amount of gallium increases to $Ga_{1.0}In_{1.0}O_{2.9}$, since the band gap of gallium oxide is ∼4.2−4.7 eV. This is consistent with previous reports and the amorphous nature of the films also suggests the formation of β-Ga_2O_3 since deposition below 650 °C typically affords amorphous gallium oxide.[13,23]

dx.doi.org/10.1021/cm102292b |*Chem. Mater.* 2011, 23, 1719–1726

Four-point probe measurements on the films deposited at 450 °C indicate that they were conductive at room temperature with an approximate sheet resistivity, R_s = 83.3 Ω/square, and low electrical resistivity values ranging from 6.66×10^{-4} Ω cm to 9.996×10^{-4} Ω cm depending on the thickness of the films. Sheet resistance is not simply dependent on the electronic properties of the material but also heavily influenced by factors such as film thickness and surface morphology. These films were found to vary in thickness from 80 to 120 nm as determined by side on SEM, with the thicker areas found at the center of the films. The resistivity value for the film with a 80 nm thickness was 6.66×10^{-4} Ω cm. These values are comparable to that of ITO, which has a resistivity of 1.5×10^{-4} Ω cm.[31] Until this report, films of In_2O_3 have not before been deposited via CVD techniques with electrical resistivity values less than $\sim 9 \times 10^{-4}$ Ω cm,[32,33] with the exception of one film deposited via electron beam evaporation which was reported to have an electrical resistivity of 2×10^{-4} Ω cm.[34] Other doped indium oxide materials with comparable electrical resistivity include In_2O_3:F with a resistivity of 2.80×10^{-4} Ω cm[35] and In_2O_3:S, 5.2×10^{-4} Ω cm,[36] which were both deposited via various CVD techniques. Unfortunately, the films deposited at temperatures below 450 °C could not be accurately analyzed using the four-point probe method due to the films being too thin.

SUMMARY

The AACVD reaction of $GaMe_3$, $InMe_3$, and an excess of $HOCH_2CH_2OMe$ in toluene yielded transparent films of gallium−indium−oxide at 350−450 °C. The composition of the resulting gallium−indium oxide films was found to vary with temperature. More gallium than indium was incorporated into the preannealed films at lower temperatures (350 °C), suggesting that the gallium species reacts more quickly at these temperatures. The films deposited on quartz at 450 °C gave the best coverage, and EDXA and WDX analysis showed that the as-deposited and annealed (at 1000 °C) films have the same composition ($Ga_{0.6}In_{1.4}O_{3.1}$). In these films, less gallium than indium has been incorporated despite the same Ga:In ratio being used in the precursor mix in all film depositions. It is possible that some gallium gets vaporized or that the higher temperature favors the formation of a gallium-substituted In_2O_3 framework (rather than a indium-substituted Ga_2O_3 framework), which is expected if $x < 1$ ($Ga_xIn_{2-x}O_3$).[9] Other precursor ratios were investigated (1:5 and 5:1 of $GaMe_3$:$InMe_3$), but the amount of Ga and In observed in the resulting films did not relate to the original precursor ratio. Moreover, these precusor ratios did not improve the films, and in fact they had inferior functional properties (conductivity, transmission) to the films described in detail herein (1:1 precursor mix).

Conductivity measurements showed films to have sheet resistivity R_s = 83.3 Ω/square and exceptionally low electrical resistivity, for example, 6.66×10^{-4} Ω cm for a 80 nm thick film. SEM images of the films annealed at 1000 °C showed individual crystallites that are evenly distributed and of the same shape. XPS of the film annealed at 1000 °C showed that the film formed is predominantly a gallium−indium−oxide material, consistent with EDXA and WDX analysis. Glancing-angle powder XRD pattern of the films annealed at 1000 °C indicated that a cubic indium oxide structure was adopted with a lattice parameter a = 9.84 Å. The lattice parameter observed is indicative of a unit cell contraction, which is consistent with the substitution of some indium atoms in the indium oxide framework with gallium atoms. AFM techniques showed films to have a variety of rms roughness values, and while some samples had a desirable rms roughness of less than 100 nm, many had higher rms roughness. In addition, a Kelvin probe measurement found the work function of the film was 4.6 eV, which is comparable to ITO.

In conclusion, transparent electrically conductive gallium−indium−oxide films have been grown for the first time via AACVD using $GaMe_3$, $InMe_3$, and $HOCH_2CH_2OMe$ in toluene at 450 °C. The in situ reaction of the reagents eliminates the need for the synthesis, isolation, and purification of a single-source metal alkoxide precursor and represents a facile method for the formation of TCO films, without the necessity of oxygen carrier gas.

ASSOCIATED CONTENT

Supporting Information. Tauc plots, raw data, and absorbance (XLS). This material is available free of charge via the Internet at http://pubs.acs.org.

AUTHOR INFORMATION

Corresponding Author

*E-mail c.j.carmalt@ucl.ac.uk; tel. +44 (0)207 6797528; fax +44 (0)207 6797463.

ACKNOWLEDGMENT

The EPSRC is thanked for a studentship (C.E.K) as well as the Platform Grant (EP/H00064X) for funding. Professor F. Cacialli and Mr. Y. Shin are thanked for AFM images and Kelvin probe experiment. SAFC Hitech is thanked for supplying $InMe_3$ and $GaMe_3$. Dr. Emily Smith (University of Nottingham) is thanked for carrying out XPS analysis under EPSRC grant EP/F019750/1: "A Coordinated Open-Access Centre for Comprehensive Materials Analysis."

REFERENCES

(1) Exarhos, G. J.; Zhou, X. D. *Thin Solid Films* **2007**, *515*, 7025.
(2) (i) Hoel, C. A.; Mason, T. O.; Gaillard, J.-F.; Poeppelmeier, K. R. *Chem. Mater.* **2010**, *22*, 3569. (ii) Freeman, A. J.; Poeppelmeier, K. R.; Mason, T. O.; Chang, R. P. H.; Marks, T. J. *MRS Bull.* **2000**, *25*, 45.
(3) Granqvist, C. G.; Hultåker, A. *Thin Solid Films* **2002**, *411*, 1.
(4) Exarhos, G. J.; Zhou, X.-D. *Thin Solid Films* **2007**, *515*, 7025–7052.
(5) Ginley, D. S.; Bright, C. *MRS Bull.* **2000**, *25*, 15.
(6) Kim, J.-S.; Cacialli, F.; Friend, R. *Thin Solid Films* **2003**, *445*, 358.
(7) (a) Minami, T. *Thin Solid Films* **2008**, *516*, 5822. (b) Ataev, B. M.; Bagamadova, A. M.; Djabrailov, A. M.; Mamedov, V. V.; Rabadanov, R. A. *Thin Solid Films* **1995**, *260*, 19.
(8) Ingram, B. J.; Gonzalez, G. B.; Kammler, D. R.; Bertoni, M. I.; Mason, T. O. *J. Electroceram.* **2004**, *13*, 167.
(9) Wang, A. C.; Edleman, N. L.; Babcock, J. R.; Marks, T. J.; Lane, M. A.; Brazis, P. R.; Kannewurf, C. R. *J. Mater. Res.* **2002**, *17*, 3155.
(10) Cava, R. J.; Phillips, J. M.; Kwo, J.; Thomas, G. A.; Vandover, R. B.; Carter, S. A.; Krajewski, J. J.; Peck, W. F.; Marshall, J. H.; Rapkine, D. H. *Appl. Phys. Lett.* **1994**, *64*, 2071.
(11) Phillips, J. M.; Kwo, J.; Thomas, G. A.; Carter, S. A.; Cava, R. J.; Hou, S. Y.; Krajewski, J. J.; Marshall, J. H.; Peck, W. F.; Rapkine, D. H.; van Dover, R. B. *Appl. Phys. Lett.* **1994**, *65*, 115.
(12) Minami, T.; Takeda, Y.; Kakumu, T.; Takata, S.; Fukuda, I. *J. Vac. Sci. Technol. A* **1997**, *15*, 958. Minami, T.; Takata, S.; Kakumu, T. *J. Vac. Sci. Technol. A* **1996**, *14*, 1689.

(13) (a) Chiang, H. Q.; Hong, D.; Hung, C. M.; Presley, R. E.; Wager, J. F.; Park, C.-H.; Keszler, D. A.; Herman, G. S. *J. Vac. Sci. Technol. A* **2006**, *24*, 2702. (b) Edwards, D. D. *J. Am. Ceram. Soc.* **1997**, *80*, 253.
(14) Jones, A. C. *J. Mater. Chem.* **2002**, *12*, 2576.
(15) Newport, A.; Carmalt, C. J.; Parkin, I. P.; O'Neill, S. A. *J. Mater. Chem.* **2002**, *12*, 1906.
(16) Basharat, S.; Carmalt, C. J.; Barnett, S. A.; Tocher, D. A.; Davies, H. O. *Inorg. Chem.* **2007**, *46*, 9473.
(17) Basharat, S.; Carmalt, C. J.; Palgrave, R.; Barnett, S. A.; Tocher, D. A.; Davies, H. O. *J. Organomet. Chem.* **2008**, *693*, 1787.
(18) Peters, E. S.; Carmalt, C. J.; Parkin, I. P. *J. Mater. Chem.* **2004**, *14*, 3474.
(19) Knapp, C. E.; Carmalt, C. J.; McMillan, P. F.; Wann, D. A.; Robertson, H. E.; Rankin, D. W. H. *Dalton Trans.* **2008**, 6880.
(20) (a) Carmalt, C. J.; King, S. J. *Coord. Chem. Rev.* **2006**, *250*, 682. (b) Bloor, L.; Pugh, D.; Carmalt, C. J. *Coord. Chem. Rev.* **2011**, doi:10.1016/j.ccr.2010.12.018.
(21) Basharat, S.; Carmalt, C. J.; Binions, R.; Palgrave, R.; Parkin, I. P. *Dalton Trans.* **2008**, 591.
(22) Basharat, S.; Carmalt, C. J.; King, S. J.; Peters, E. S.; Tocher, D. A. *Dalton Trans.* **2004**, 3475.
(23) Binions, R.; Carmalt, C. J.; Parkin, I. P.; Pratt, K. F. E.; Shaw, G. A. *Chem. Mater.* **2004**, *16*, 2489.
(24) Knapp, C. E.; Pemberton, L.; Carmalt, C. J.; Pugh, D.; McMillan, P. F.; Barnett, S. A; Tocher, D. A. *Main Group Chem.* **2010**, *9*, 31–40.
(25) Mareizo, M. *Acta Crystallogr.* **1966**, *20*, 723.
(26) Mareizo, M.; Remeika, J. P. *J. Chem. Phys.* **1967**, *46*, 1862.
(27) Shannon, R. D. *Acta Crystallogr., Sect. A* **1976**, *32*, 751.
(28) Suh, S.; Hoffman, D. M. *J. Am. Chem. Soc.* **2000**, *122*, 9396.
(29) Chi, Y.; Chou, T. Y.; Wang, Y. J.; Huang, S. F.; Carty, A. J.; Scoles, L.; Udachin, K. A.; Peng, S. M.; Lee, G. H. *Organometallics* **2004**, *23*, 95.
(30) Tauc, J. *Mater. Res. Bull.* **1968**, *3*, 37.
(31) Vossen, J. L. *Phys. Thin Films* **1977**, *9*, 1.
(32) Korzo, V. F.; Chernyaev, V. N. *Phys. Status Solidi A* **1973**, *20*, 695.
(33) Mayer, B. *Thin Solid Films* **1992**, *221*, 166.
(34) Pan, C. A.; Ma, T. P. *J. Electron. Mater.* **1981**, *10*, 43.
(35) Maruyama, T.; Fukki, K. *Jpn. J. Appl. Phys.* **1990**, *29*, L1705.
(36) Ryoki, N.; Kazuhisa, K.; Haruo, M. *J. Electrochem. Soc.* **1991**, *138*, 631.